SOI: 1.1/TAS DOI: 10.15863/TAS
International Scientific Journal
Theoretical & Applied Science

p-ISSN: 2308-4944 (print) **e-ISSN:** 2409-0085 (online)

Year: 2021 **Issue:** 05 **Volume:** 97

Published: 30.05.2021 **http://T-Science.org**

QR – Issue QR – Article

Denis Chemezov
Vladimir Industrial College
M.Sc.Eng., Corresponding Member of International Academy
of Theoretical and Applied Sciences, Lecturer, Russian Federation
https://orcid.org/0000-0002-2747-552X
vic-science@yandex.ru

Petr German
Vladimir Industrial College
Student, Russian Federation

Danil Zubatov
Vladimir Industrial College
Student, Russian Federation

Aleksey Kuzin
Vladimir Industrial College
Student, Russian Federation

Emil Akhmetov
Vladimir Industrial College
Student, Russian Federation

Artem Gorechnin
Vladimir Industrial College
Student, Russian Federation

Georgiy Karatun
Vladimir Industrial College
Student, Russian Federation

COMPARISON OF THE BULLET PENETRATION WHEN SHOOTING FROM THE AK-109 ASSAULT RIFLE AT THE TARGETS MADE OF VARIOUS METALLIC AND NON-METALLIC MATERIALS

***Abstract**: The results of modeling the bullet penetration of the AK-109 assault rifle into the targets made of Kevlar, high-strength concrete, stainless steel, aluminum alloy, thermopolished glass and titanium alloy are presented in the article. An idea of the failure degree of metallic and non-metallic materials when shooting from the assault rifle is given. It was determined that under the same conditions of shooting, the targets made of titanium alloy showed maximum strength.*

***Key words**: the bullet, the target, the penetration depth, destruction, elastic and plastic deformations.*
***Language**: English*
***Citation**: Chemezov, D., et al. (2021). Comparison of the bullet penetration when shooting from the AK-109 assault rifle at the targets made of various metallic and non-metallic materials. *ISJ Theoretical & Applied Science, 05 (97),* 581-593.
Soi: http://s-o-i.org/1.1/TAS-05-97-90 ***Doi***: crossref https://dx.doi.org/10.15863/TAS.2021.05.97.90

Introduction

The firearm is the weapon designed to mechanically defeat of the target at the distance by the projectile that receives directional movement due to the energy of the powder or other charge [1]. Automatic small arms, called the assault rifles, are used to create high-density fire and the targets defeat at the short distances. The reliability and the simplicity of the design of the Kalashnikov assault rifle make it the most common small arms in the world [2].

The 5.45mm and 7.62mm cartridges are used for shooting, depending on the modification of the Kalashnikov assault rifle. The 7.62mm cartridge considered in this work is used for shooting from the AK-109 assault rifle. The cartridge consists of the bullet, the case, the powder charge, and the percussion cap. The general view of the 3D model of the 7.62mm cartridge for the AK-109 assault rifle is presented in the Fig. 1.

Figure 1 – The 3D model of the 7.62mm cartridge for the AK-109 assault rifle.

The initial flight speed of the steel bullet is 700-720 m/s. The high flight speed and the design of the assault rifle bullet allow you to fire with high striking ability. One of the characteristics of striking ability of the bullet is the penetrating ability, which is determined by the path traveled by the bullet along the ballistic trajectory in the targets made of various materials [3-5]. It depends on the characteristics of the moving bullet. The values of the bullet penetration of the assault rifle into the metallic, brick, glass, wood, concrete and other targets were determined experimentally (under the normal conditions). However, the analysis of the deformation degree, cracking and destruction of materials can be done after the thorough examination in the laboratory. To reduce the time of testing and the laboratory examinations, it is rational to carry out shooting from the assault rifle and the analysis of the stress and strain state of the target materials by the method of finite element modeling in special software products.

2. Materials and methods

2.1. Modeling conditions

The computer simulation [6] of the process of shooting from the AK-109 assault rifle at the targets was implemented in the ANSYS Autodyn 14.5 program. The process simulation of penetration of the bullet model at the angle of 90 degrees into the targets models made of various metallic and non-metallic materials was the two-dimensional statement of the study. The initial velocity (v) of the bullet flight along the X-axis was adopted 720 m/s. The target was the plate fixed on one of the sides. The bullet and target models were divided into 1250 and 3500 finite elements, respectively [7]. The interaction between the bullet and the target was carried out by the Lagrange/Lagrange solver. The external gap during the contact was determined by the value of 0.008741. The safety factor in the conditions of deformation of the bullet and target models was adopted 0.2. The statement of the modeling process of the bullet penetration of the assault rifle into the target is presented in the Fig. 2.

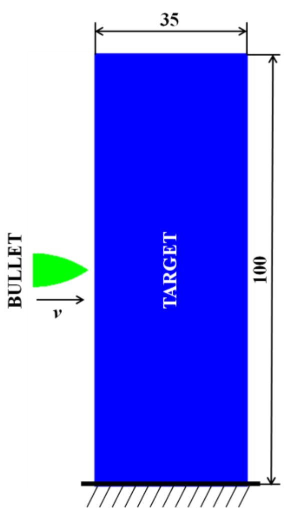

Figure 2 – The statement of the modeling process of shooting at the target.

The bullet and targets models were given the properties of carbon steel, Kevlar, high-strength concrete, stainless steel, aluminum alloy, thermopolished glass, and titanium alloy.

2.2. The properties of 1006 carbon steel (the bullet material)

1006 carbon steel is steel containing mainly carbon as the alloying element. It contains about 0.4% silicon and 1.2% manganese. Chromium, nickel, aluminum, copper and molybdenum are also present in small quantities in carbon steel. The features of AISI 1006 carbon steel are mainly softness and ductility. 1006 carbon steel was adopted for the bullet model of the assault rifle. The material density is 7.896 g/cm^3. The following parameters were set for the material state: the equation – shock; the Gruneisen coefficient – 2.17; the parameter *C1* – 4.569×10^3 m/s; the parameter *S1* – 1.49; the reference temperature – 300 K; the specific heat – 451.999969 J/(kg×K). The strength characteristics of material were set by the following parameters: the type of the strength model – Johnson-Cook; the shear modulus – 8.180001×10^7 kPa; yield stress – 3.5×10^5 kPa; the hardening constant – 2.75×10^5 kPa; the hardening exponent – 0.36; the strain rate constant – 0.022; the thermal softening exponent – 1.0; the melting temperature – 1.811×10^3 K; the reference strain rate (/s) – 1.0; the strain rate correction – 1st order.

2.3. The properties of Kevlar/epoxy composite (the first material of the target)

Kevlar is the heat-resistant and strong synthetic fiber, related to other aramids [8]. In unidirectional Kevlar/epoxy composite, the modular ratio is 20 and epoxy occupies 60% of the volume. This material was adopted for the target No. 1. The material density is 1.65 g/cm^3. The following parameters were set for the material state: the equation – orthotropic; stiffness – the stiffness matrix; *C11* – 3.425001×10^6 kPa; *C22* – 1.35×10^7 kPa; *C33* – 1.35×10^7 kPa; *C12* – 1.14×10^6 kPa; *C23* – 1.2×10^6 kPa; *C31* – 1.14×10^6 kPa; the shear modulus 12 – 1.0×10^6 kPa; the shear modulus 23 – 1.0×10^6 kPa; the shear modulus 31 – 1.0×10^6 kPa; the material axes – the *X-Y-Z* space; the *Z*-coordinate for the direction 11 (*XYZ*) – 1 mm; the volumetric response – polynomial; the bulk modulus *A1* – 4.153889×10^6 kPa; the parameter *A2* – 4.000001×10^7 kPa; the parameter *T1* – 4.153889×10^6 kPa; the reference temperature – 300 K; the specific heat – 1.42×10^3 J/(kg×K). The strength characteristics of material were set by the following parameters: the type of the strength model – elastic; the shear modulus – 1.0×10^6 kPa. The process of material failure during deformation was carried out according to the following specified parameters: the type of the failure model – material stress/strain; tensile failure stress 11 – 1.0×10^{20} kPa; tensile failure stress 22 – 1.0×10^{20} kPa; tensile failure stress 33 – 1.0×10^{20} kPa; maximum shear stress 12 – 1.0×10^{20} kPa; maximum shear stress 23 – 1.01×10^{20} kPa; maximum shear stress 31 – 1.01×10^{20} kPa; tensile failure strain 11 – 0.01; tensile failure strain 22 – 0.08; tensile failure strain 33 – 0.08; maximum shear strain 12 – 1.0×10^{20}; maximum shear strain 23 – 1.01×10^{20}; maximum shear strain 31 – 1.01×10^{20}; the material axes option – the *IJK* space; the post failure option – orthotropic; the residual shear stiffness fraction – 0.2; maximum residual shear stress – 1.0×10^{20} kPa; the decomposition temperature – 700 K; the matrix melt temperature – 1.01×10^{20} K; failed in 11, the failure mode – 11 only; failed in 22, the failure mode – 22 only; failed in 33, the failure mode – 33 only; failed in 12, the failure mode – 12 & 11 only; failed in 23, the failure mode – 23 & 11 only; failed in 31, the failure mode – 31 & 11 only; the melt matrix failure mode – bulk.

2.4. The properties of 140 MPa compressive strength concrete (the second material of the target)

Concrete is composite material composed of fine and coarse aggregate bonded together with fluid cement (the cement paste) that hardens (cures) over time [9]. Concrete is high-strength (it has compressive strength greater than 40 MPa). This material was adopted for the target No. 2. The material density is 2.75 g/cm^3. The following parameters were set for the material state: the equation – *P* alpha; the porous density – 2.52 g/cm^3; the porous sound speed – 3.242×10^3 m/s; initial compaction pressure – 9.33×10^4 kPa; solid compaction pressure – 6.0×10^6 kPa; the compaction exponent – 3.0; the solid *EOS* – polynomial; the bulk modulus *A1* – 3.527×10^7 kPa; the parameter *A2* – 3.958×10^7 kPa; the parameter *A3* – 9.04×10^6 kPa; the parameter *B0* – 1.22; the parameter *B1* – 1.22; the parameter *T1* – 3.527×10^7 kPa; the reference temperature – 300 K; the specific heat – 653.999939 J/(kg×K); the compaction curve – standard. The strength characteristics of material were set by the following parameters: the type of the strength model – *RHT* concrete; the shear modulus – 2.206×10^7 kPa; compressive strength (*fc*) – 1.4×10^5 kPa; tensile strength (*ft/fc*) – 0.1; shear strength (*fs/fc*) – 0.18; the intact failure surface constant *A* – 1.6; the intact failure surface exponent *N* – 0.61; the tens./comp. meridian ratio (*Q*) – 0.6805; brittle to ductile transition – 0.0105; *G* (elas.)/(elas.-plas.) – 2.0; elastic strength/*ft* – 0.7; elastic strength/*fc* – 0.53; the fractured strength constant *B* – 1.6; the fractured strength exponent *M* – 0.61; the compressive strain rate exp. alpha – 0.00909; the tensile strain rate exp. delta – 0.0125; the maximum fracture strength ratio – 1.0×10^{20}; use *CAP* on the elastic surface – yes. The process of material failure during deformation was carried out according to the following specified parameters: the type of the failure model – *RHT* concrete; the damage constant, *D1* – 0.04; the damage constant, *D2* – 1.0; minimum strain to failure – 0.01; the residual shear modulus fraction – 0.13; tensile failure – hydro (P_{min}). Material was given the numerical mechanism to automatically removing the elements during the simulation: the type of the erosion model – geometric strain; erosion strain – 2.0; the type of geometric strain – instantaneous.

2.5. The properties of 304 stainless steel (the third material of the target)

SAE 304 stainless steel is the most common stainless steel [10]. Steel contains both chromium (between 18% and 20%) and nickel (between 8% and 10.5%) metals as main non-iron constituents. It is austenitic stainless steel. This material was adopted for the target No. 3. The material density is 7.9 g/cm^3. The following parameters were set for the material state: the equation – shock; the Gruneisen coefficient – 1.93; the parameter *C1* – 4.57×10^3 m/s; the parameter *S1* – 1.49; the reference temperature – 300 K; the specific heat – 422.999939 J/(kg×K). The strength characteristics of material were set by the following parameters: the type of the strength model – Steinberg-Guinan; the shear modulus – 7.7×10^7 kPa; yield stress – 3.4×10^5 kPa; maximum yield stress – 2.5×10^6 kPa; the hardening constant – 43; the hardening exponent – 0.35; the derivative dG/dP – 1.74; the derivative dG/dT – -3.504×10^4 kPa/K; the derivative dY/dP – 0.007684; the melting temperature – 2.38×10^3 K.

2.6. The properties of 2024 aluminum alloy (the fourth material of the target)

2024 aluminum alloy is aluminum alloy, with copper as the primary alloying element [11]. It is used in applications requiring high strength to the weight ratio, as well as good fatigue resistance. This material was adopted for the target No. 4. The material density is 2.785 g/cm^3. The following parameters were set for the material state: the equation – shock; the Gruneisen coefficient – 2.0; the parameter *C1* – 5.328×10^3 m/s; the parameter *S1* – 1.338.

2.7. The properties of float glass (the fifth material of the target)

Float glass is the sheet of glass made by floating molten glass on the bed of molten metal, typically tin, although lead and other various low-melting-point alloys [12]. This method gives the sheet uniform thickness and very flat surfaces. This material was adopted for the target No. 5. The material density is 2.53 g/cm^3. The following parameters were set for the material state: the equation – polynomial; the bulk modulus *A1* – 4.54×10^7 kPa; the parameter *A2* – -1.38×10^8 kPa; the parameter *A3* – 2.9×10^8 kPa; the parameter *T1* – 4.54×10^7 kPa. The strength characteristics of material were set by the following parameters: the type of the strength model – Johnson-Holmquist; the shear modulus – 3.04×10^7 kPa; the model type – continuous (*JH2*); the Hugoniot elastic limit – 5.95×10^6 kPa; the intact strength constant *A* – 0.93; the intact strength exponent *N* – 0.77; the strain rate constant *C* – 0.003; the fractured strength constant *B* – 0.35; the fractured strength exponent *M* – 0.4; the maximum fracture strength ratio – 0.5. The process of material failure during deformation was carried out according to the following specified parameters: the type of the failure model – Johnson-Holmquist; the hydro tensile limit – -3.5×10^4 kPa; the model type – continuous (*JH2*); the damage constant, *D1* – 0.053; the damage constant, *D2* – 0.85; the bulking constant, beta – 1.0; the damage type – gradual (*JH2*); tensile failure – hydro (P_{min}).

2.8. The properties of Ti-6Al-4V titanium alloy (the sixth material of the target)

Ti-6Al-4V is alpha-beta titanium alloy with high specific strength and excellent corrosion resistance. It is one of the most commonly used titanium alloys and is applied in the wide range of applications where the low density and excellent corrosion resistance are necessary such as e.g. aerospace industry and biomechanical applications. This material was adopted for the target No. 6. The material density is 4.45 g/cm^3. The following parameters were set for the material state: the equation – puff; the parameter *A1* – 9.940001×10^7 kPa; the parameter *A2* – 1.244×10^8 kPa; the parameter *A3* – 4.847×10^7 kPa; the Gruneisen coefficient – 1.0; the expansion coefficient – 0.67; the sublimation energy – 2.71×10^6 J/kg; the reference temperature – 300 K; the specific heat – 525 J/(kg×K). The strength characteristics of material were set by the following parameters: the type of the strength model – von Mises; the shear modulus – 5.5×10^7 kPa; yield stress – 1.5×10^6 kPa. The process of material failure during deformation was carried out according to the following specified parameters: the type of the failure model – hydro (P_{min}); the hydro tensile limit – -3.0×10^6 kPa; the reheal – yes; stochastic failure – yes; the stochastic variance (gamma) – 16; the minimum fail fraction – 0.1; the distribution type – the fixed seed.

3. Results and discussion

The dynamics process of the bullet penetration of the assault rifle into the target made of Kevlar/epoxy composite is presented in the Fig. 3. The target model was presented in the form of the finite elements inscribed into the dimensional rectangle. This allowed us to obtain the complete pattern of deformation of the target material during the bullet penetration. The results were recorded every 1200 cycles (0.002633 ms) of calculating the dynamics process of flight (movement) and penetration of the bullet into the target.

The penetration process is accompanied by crumpling the bullet (reducing the length and increasing the cross-section) and the formation of the blind hole in the target.

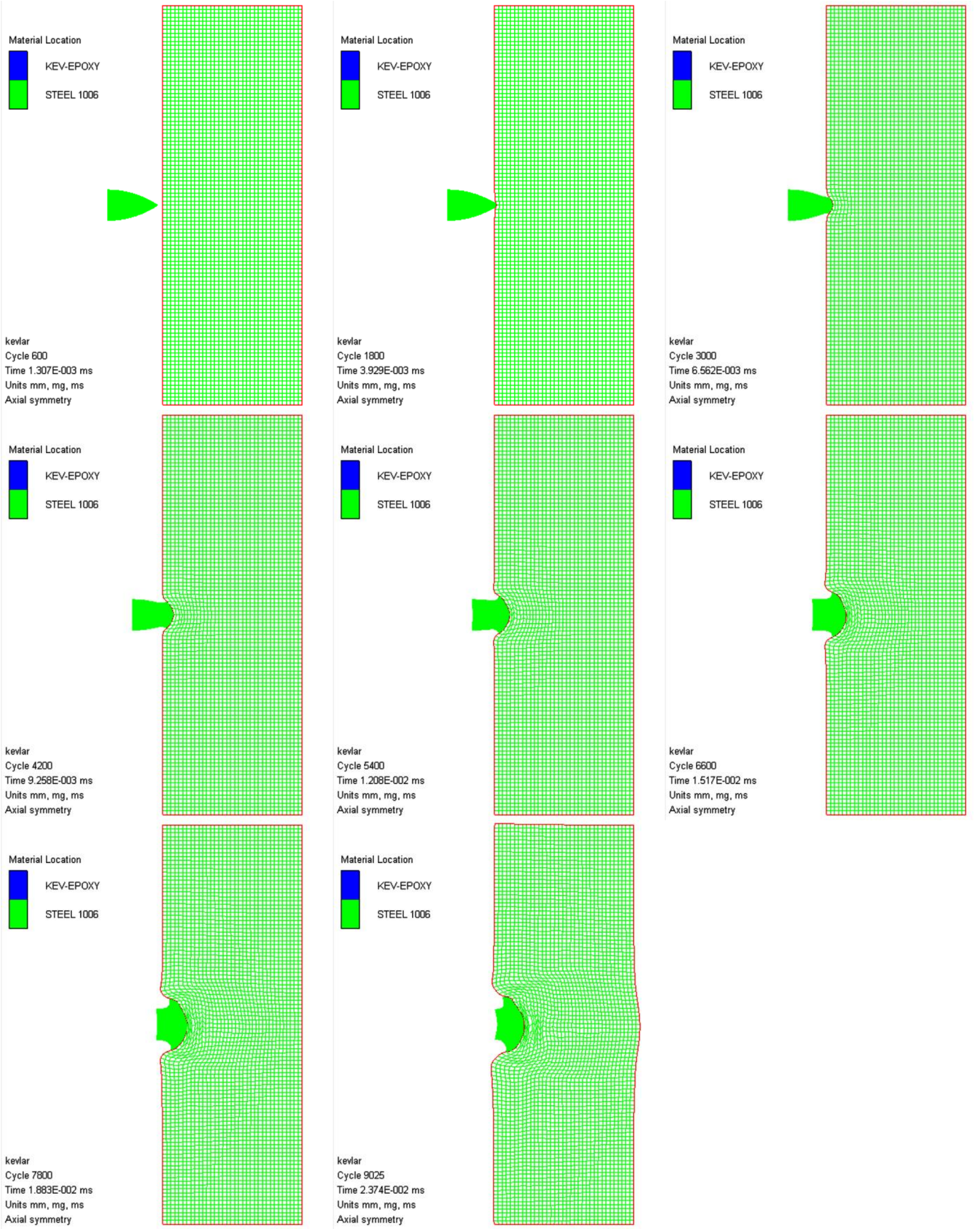

Figure 3 – The dynamics process of the bullet penetration of the assault rifle into the target made of Kevlar/epoxy composite.

It is determined that at the maximum bullet penetration (the bullet length is 14 mm), the target is bent on the reverse side. The target material in the contact zone with the bullet is significantly deformed (the maximum stretched and compressed finite elements of the target model). The images and the values of the bullet penetration into the targets made of various materials are presented in the Fig. 4 and in the table 1. The bullet is deformed in the same way during penetration into the targets made of stainless steel and thermopolished glass. The density of thermopolished glass is three times less than that of stainless steel. Maximum deformation of the bullet occurs during penetration into the target made of titanium alloy. In accordance with the scales plotted on two coordinate axes, the maximum values of the bullet penetration into the targets were determined. Shooting at the target made of titanium alloy is characterized by the minimum depth of the bullet penetration, equal to 2 mm. Similar shooting at the target made of aluminum alloy is characterized by the maximum depth of the bullet penetration, equal to 15 mm.

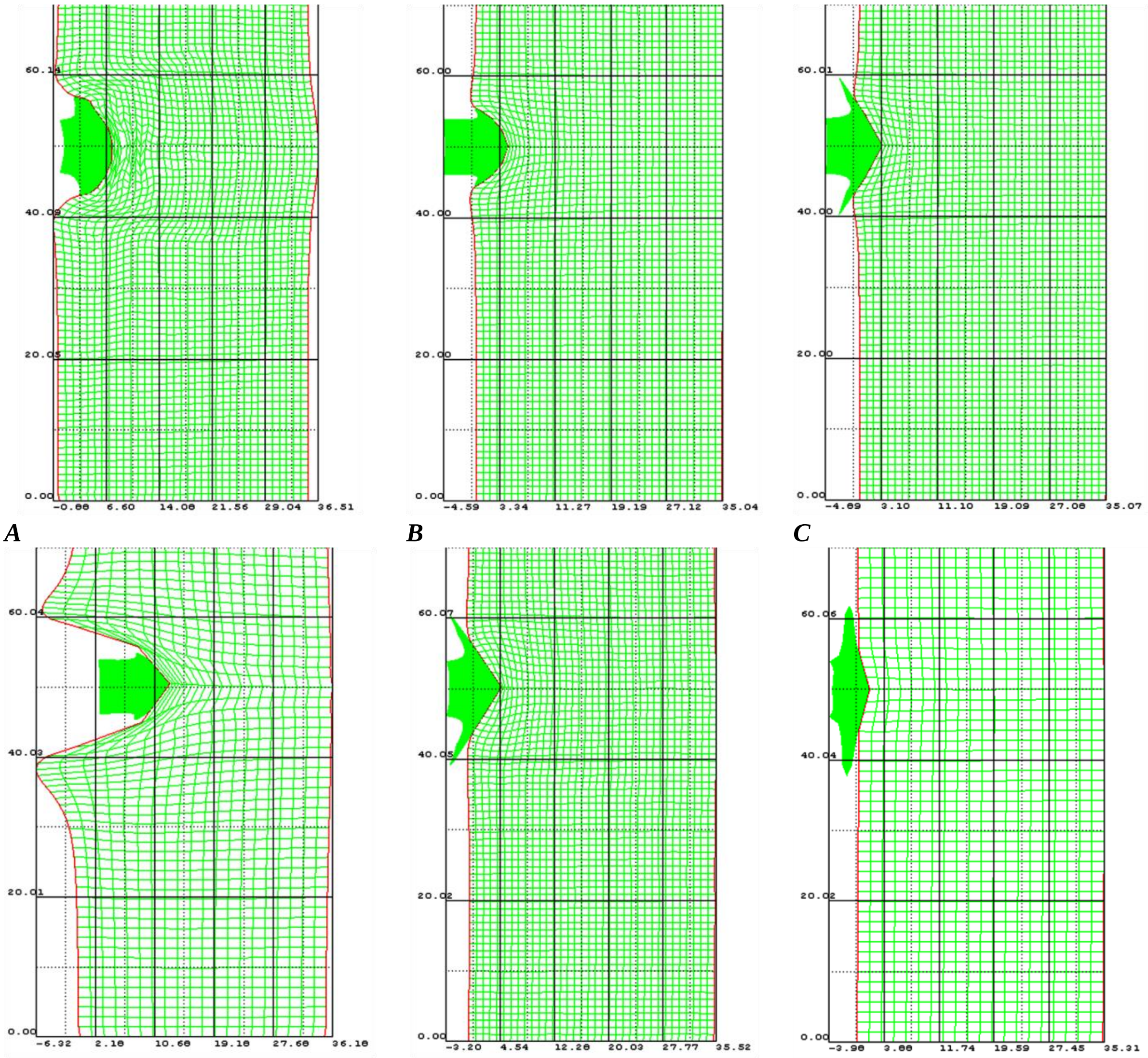

A B C D E F

Figure 4 – The penetration depth of the steel bullet into the targets made of Kevlar/epoxy composite (*A*), 140 MPa compressive strength concrete (*B*), 304 stainless steel (*C*), 2024 aluminum alloy (*D*), float glass (*E*), and Ti-6Al-4V titanium alloy (*F*).

Table 1. The values of the maximum depth of the bullet penetration into the targets, in mm.

Target material	***Kevlar/epoxy composite***	***140 MPa compressive strength concrete***	***304 stainless steel***	***2024 aluminum alloy***	***Float glass***	***Ti-6Al-4V titanium alloy***
Maximum depth of bullet penetration, mm	8.0	4.7	3.1	15.0	4.5	2.0

The state of the steel bullet and the targets made of various materials is presented in the Fig. 5. The velocity vectors of material displacement of the bullet and the targets made of various materials are presented in the Fig. 6. The contours of effective strain of the steel bullet and the targets made of various materials are presented in the Fig. 7. The contours of compression of the steel bullet and the targets made of various materials are presented in the Fig. 8. The contours of pressure in the steel bullet and the targets made of various materials are presented in the Fig. 9.

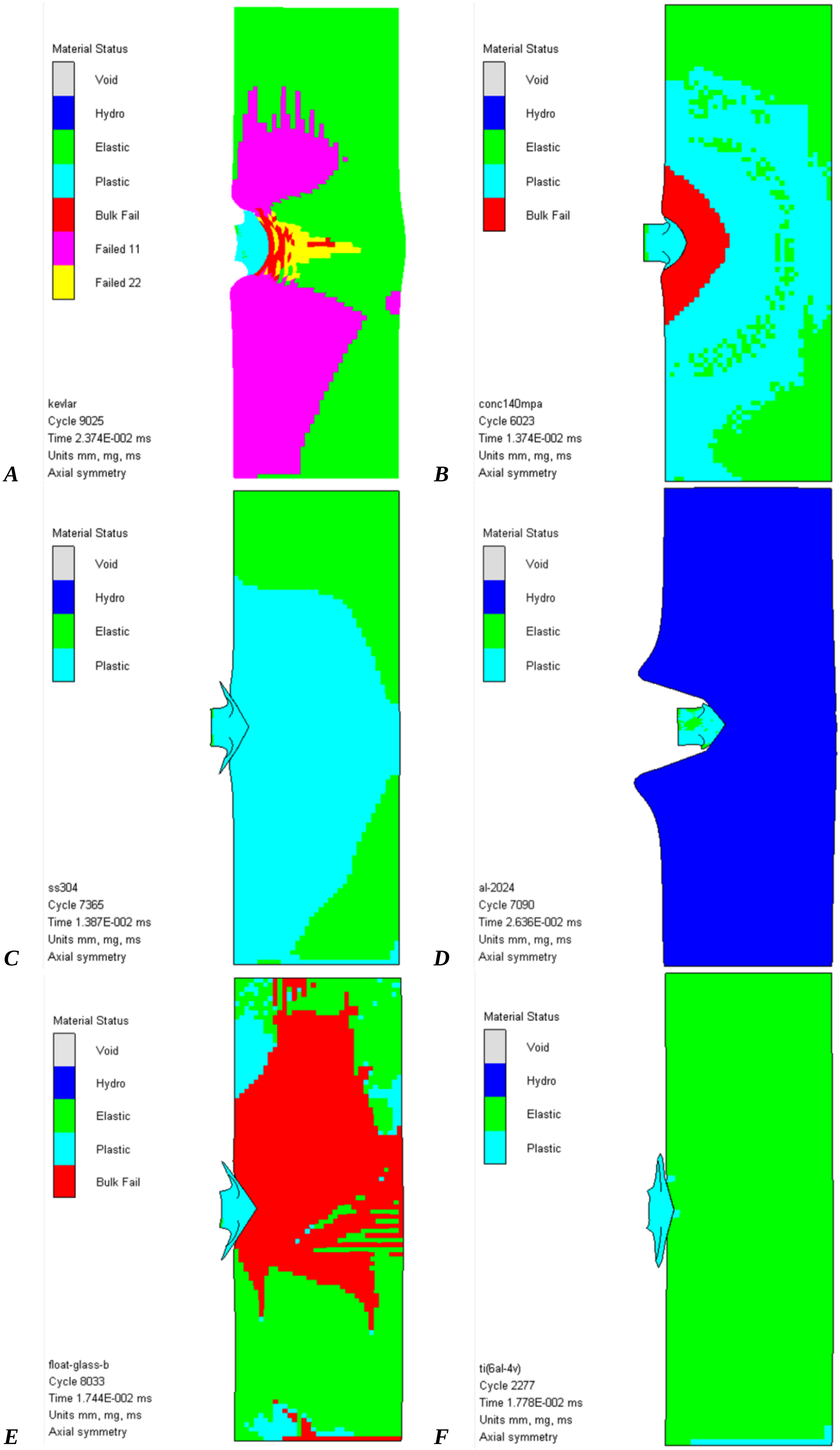

Figure 5 – The state of the steel bullet and the targets made of Kevlar/epoxy composite (*A*), 140 MPa compressive strength concrete (*B*), 304 stainless steel (*C*), 2024 aluminum alloy (*D*), float glass (*E*), and Ti-6Al-4V titanium alloy (*F*) after the simulation.

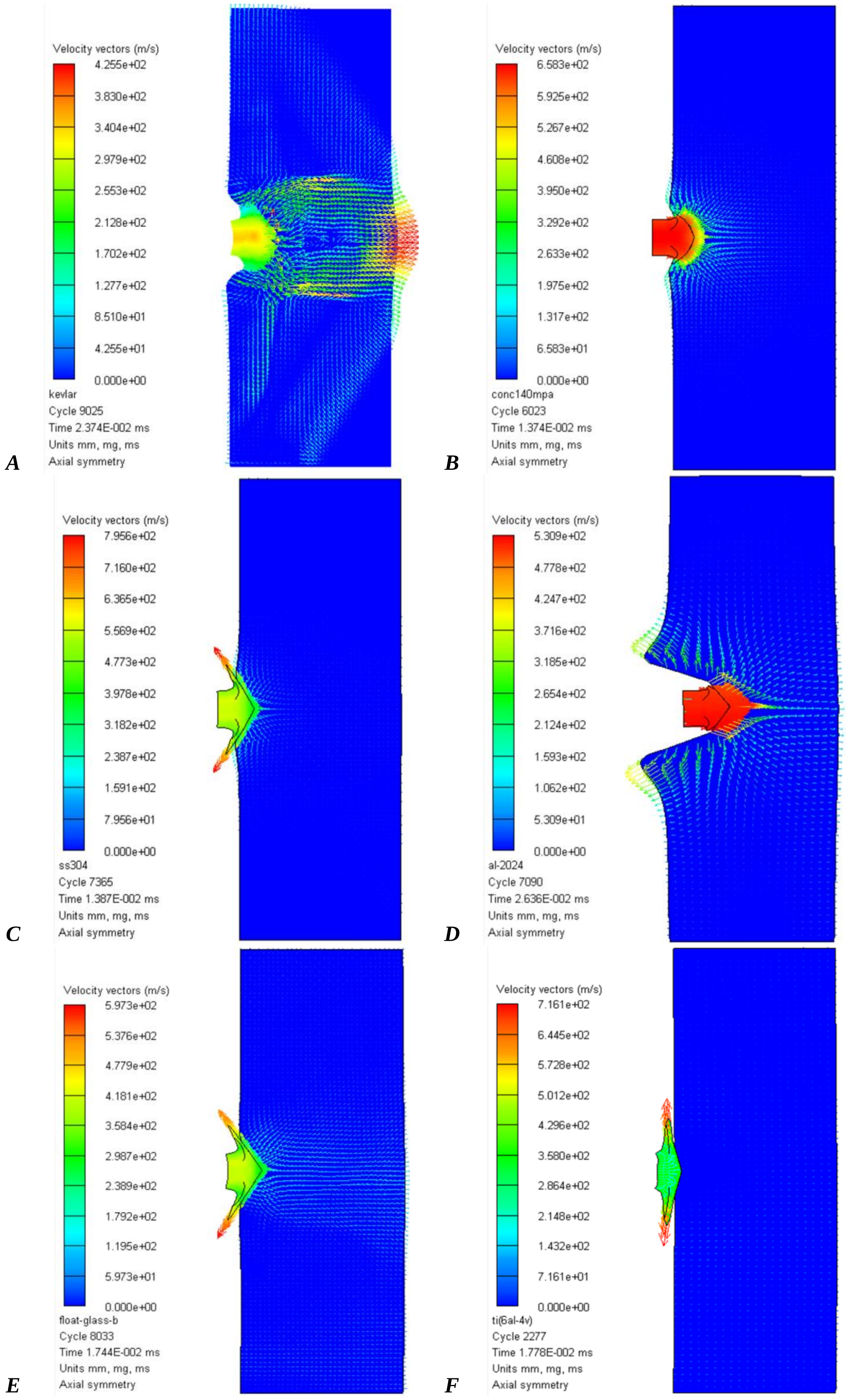

Figure 6 – The velocity vectors of material displacement of the bullet and the targets made of Kevlar/epoxy composite (*A*), 140 MPa compressive strength concrete (*B*), 304 stainless steel (*C*), 2024 aluminum alloy (*D*), float glass (*E*), and Ti-6Al-4V titanium alloy (*F*) after the simulation.

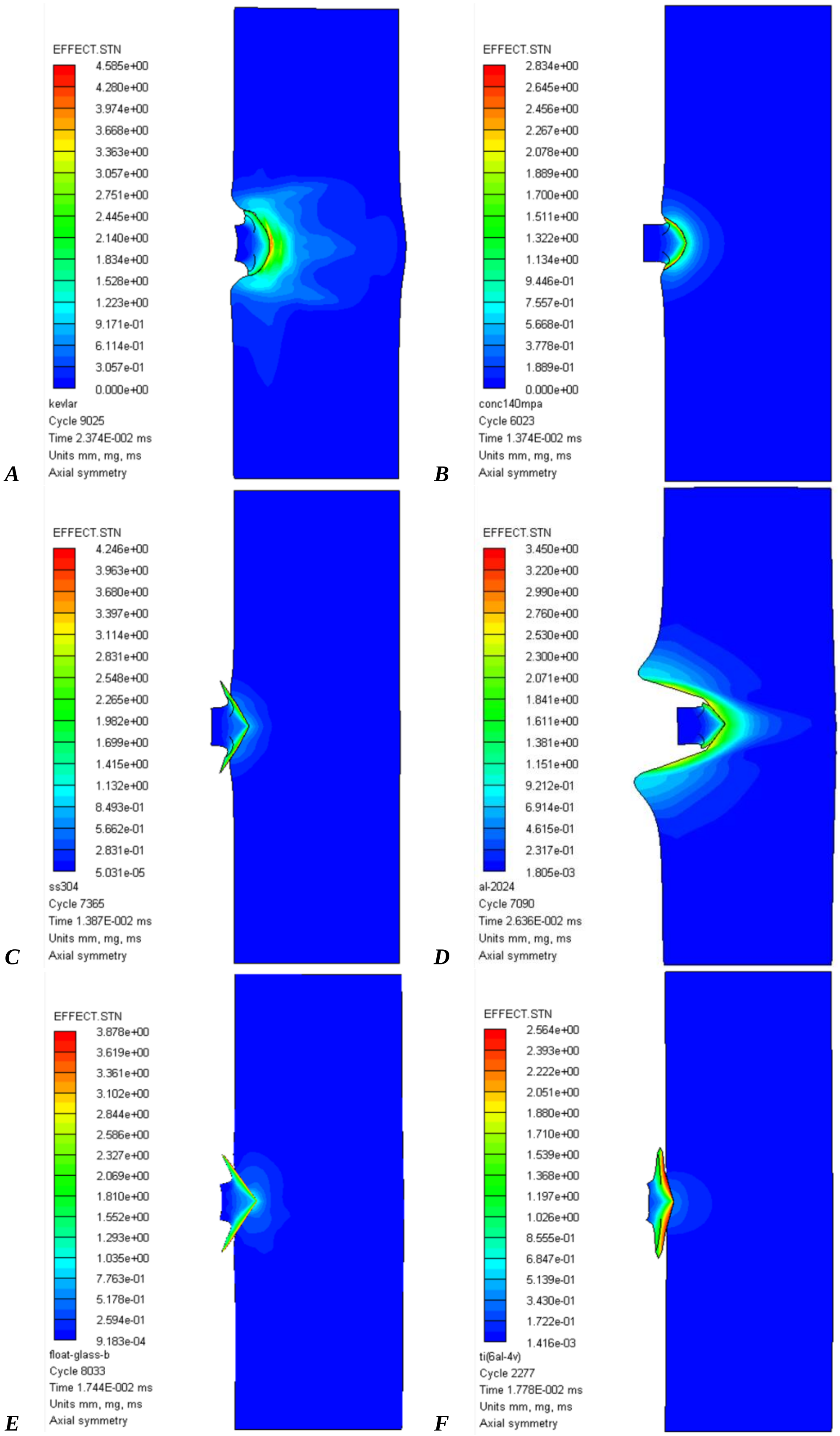

Figure 7 – The contours of effective strain of the steel bullet and the targets made of Kevlar/epoxy composite (*A*), 140 MPa compressive strength concrete (*B*), 304 stainless steel (*C*), 2024 aluminum alloy (*D*), float glass (*E*), and Ti-6Al-4V titanium alloy (*F*) after the simulation.

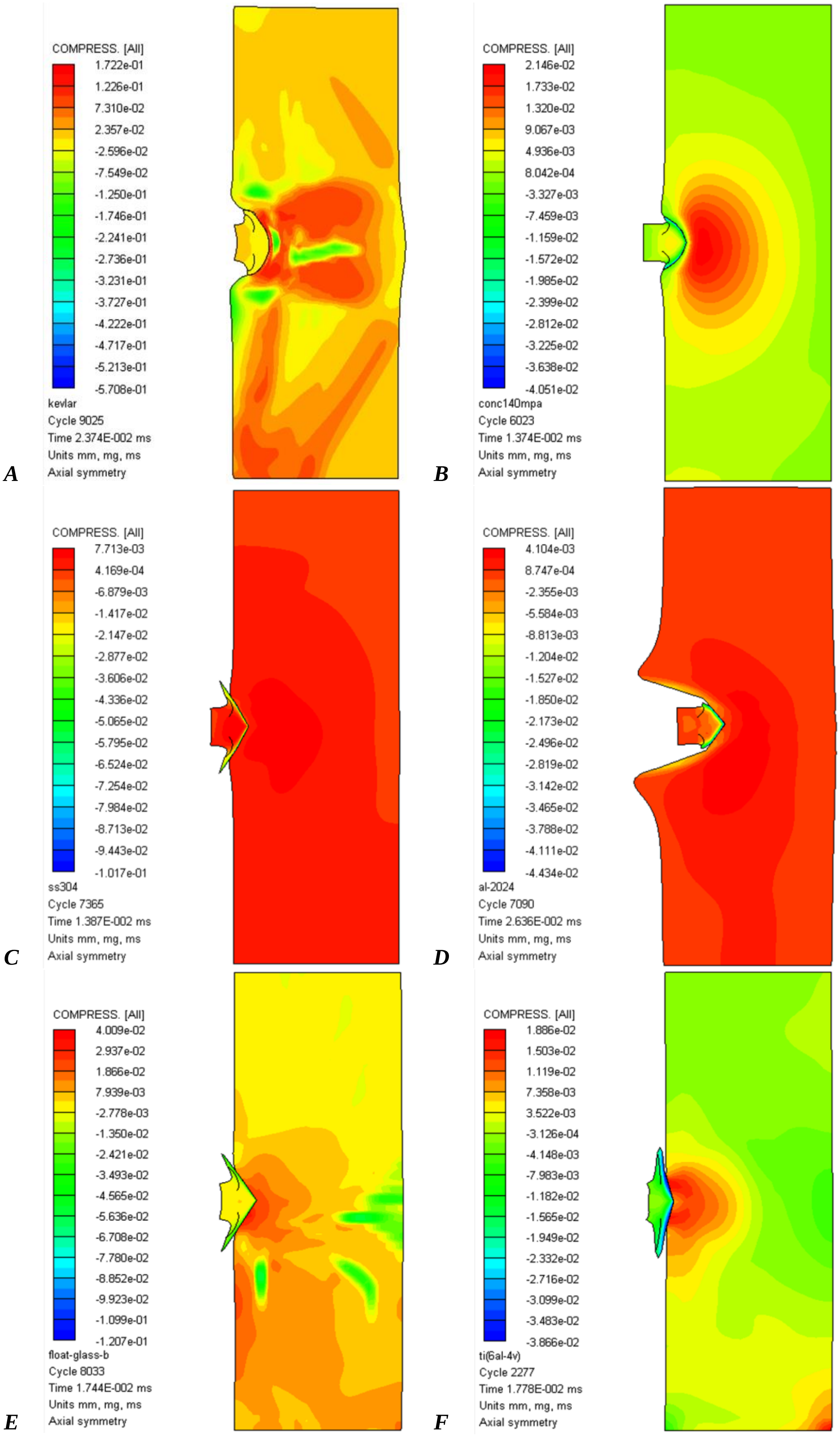

Figure 8 – The contours of compression of the steel bullet and the targets made of Kevlar/epoxy composite (*A*), 140 MPa compressive strength concrete (*B*), 304 stainless steel (*C*), 2024 aluminum alloy (*D*), float glass (*E*), and Ti-6Al-4V titanium alloy (*F*) after the simulation.

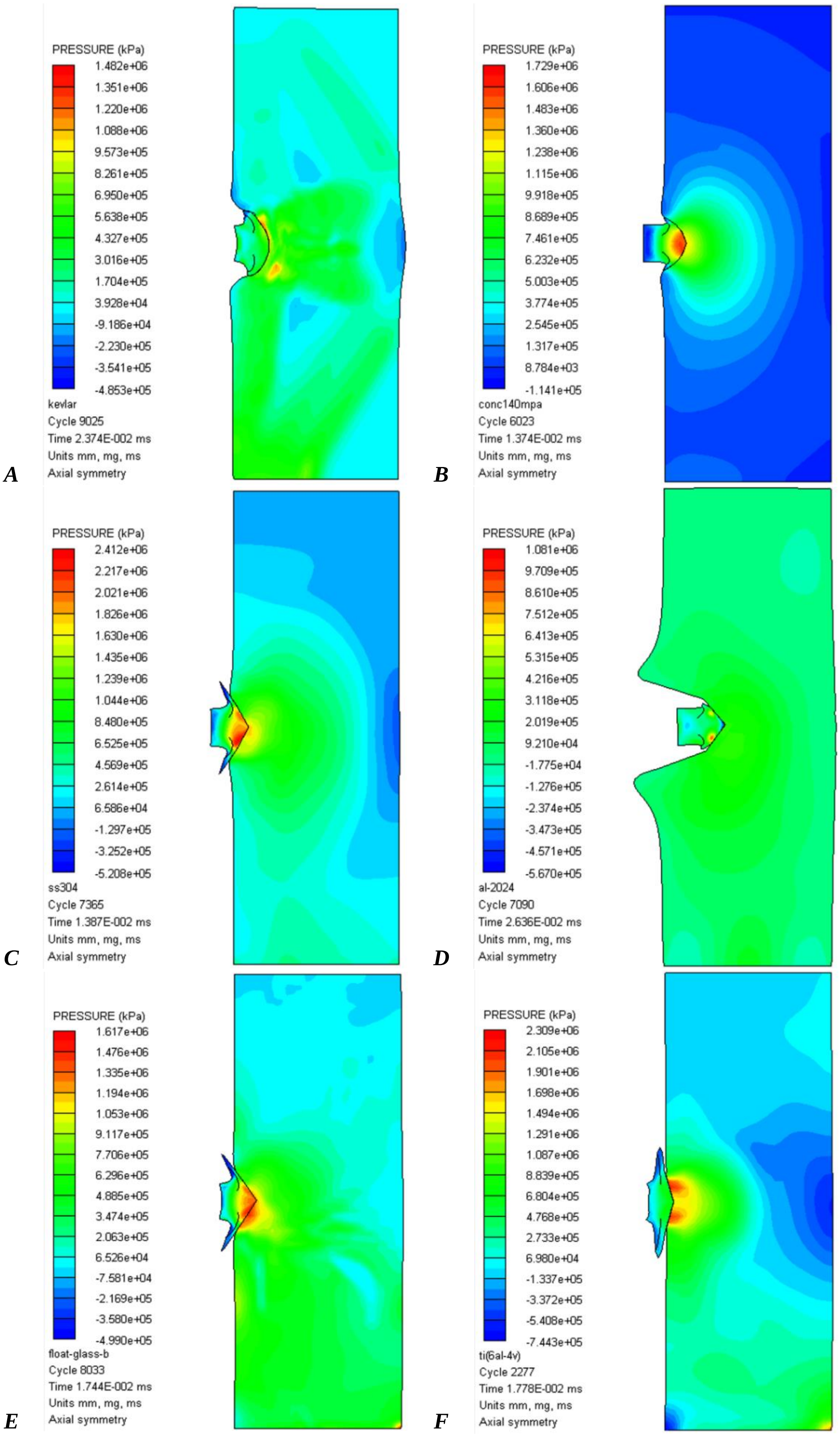

Figure 9 – The contours of pressure in the steel bullet and the targets made of Kevlar/epoxy composite (*A*), 140 MPa compressive strength concrete (*B*), 304 stainless steel (*C*), 2024 aluminum alloy (*D*), float glass (*E*), and Ti-6Al-4V titanium alloy (*F*) after the simulation.

The state of the bullet and the targets after the dynamic impact was calculated from the properties of materials. In all cases, the bullet material is subjected to plastic (changing the shape) and elastic (without changing the shape) deformations. The targets made of metallic alloys are also subjected to elastic and plastic deformations. For example, plastic deformations in titanium alloy after the bullet penetration are only 5%, and elastic deformations in stainless steel are about 40%. Thus, damage of the steel target is 12 times greater than that of the titanium target. The information about the state of the target made of aluminum alloy is not available due to the adopted properties of the model from the standard library of materials of the ANSYS Autodyn 14.5 program. The volume of destroyed material (about 8%) is formed in the contact zone of the bullet with Kevlar. There is no plastic deformation, but there are the failed volumes of material defined by two coordinate axes. The target will not change its original dimensions and the geometric shape due to elastic deformations after removing the dynamic load. High-strength concrete is characterized by the volume destruction in the impact zone of the dynamic concentrated load. The remaining volume of concrete is subjected to elastic and plastic deformations. Due to the protective layer of thermopolished glass, the bullet penetrates into the target to the depth equal to ½ of the bullet length. However, this leads to extensive destruction of material (at least 50% of the volume). It is possible to the target destruction, since this deformation is determined over the entire cross-section of the model. Elastic and plastic deformations of material are also observed. Elastic deformations prevail.

The velocity vectors determine the value and the direction of materials displacement during the bullet penetration. The displacement velocity of the target made of titanium alloy is uniform throughout the entire volume. The maximum displacement velocity is calculated for the target made of Kevlar. In this case, the displacement velocity of material in the contact zone with the bullet is less than the displacement velocity of material from the reverse convex side of the target. The uniform displacement velocity of the local volumes of the targets is observed for other materials.

The target made of Kevlar is subjected to maximum deformation, distributed on ⅓ of the model volume. Effective strain of damaged Kevlar can reach the value of 3.7. For other materials, this indicator is at least 2 times less. Minimum effective strain is observed during damage of the targets made of titanium alloy and high-strength concrete.

The contours of compression show the volumes of materials that are subject to compression deformation. In all cases, the material compression gradient zones are located behind the deformed bullet. The maximum value of compression was determined for damaged Kevlar, and the minimum value was determined for damaged aluminum alloy.

The contours of pressure determine the operating load per unit area of the target material. In the impact zone of the load in the target made of stainless steel, maximum calculated pressure of 2.021×10^6 kPa occurs. Aluminum alloy is destroyed under the pressure action of 3.118×10^5 kPa. Based on the calculated contours of pressure, it is determined that high-strength concrete has higher resistance to the dynamic loads compared to other considered materials.

4. Conclusion

The maximum depth of the bullet penetration is observed during shooting from the AK-109 assault rifle at the target made of aluminum alloy. However, the value of volumetric deformation of the aluminum plate (changing the geometric shape) after the bullet penetration is less than that of the plate made of Kevlar. Taking into account that the kevlar fabric is used for the body armor, deformation of this material at the high rate can lead to serious damage to organs and tissues of the human body. The most optimal choice of material for the body armor is titanium alloy, which is subjected to less deformation at the distance of up to 10 mm and destruction at the distance of up to 2 mm from the side of the bullet penetration. The volume of thermopolished glass is destroyed by about 50% after the bullet penetration. Destruction of high-strength concrete occurs at the distance of up to 10 mm from the deformed bullet along all coordinate axes. Thus, it can be concluded that stainless steel and titanium alloy have high strength when the bullet penetration.

References:

1. (2018). *GOST 28653-2018. Small-arms. Terms and definitions.*
2. (2019). *Ballistic Testing Recommended. AK-47 (Kalashnikov) assault rifle rounds*. Centre for the Protection of National Infrastructure, 5 p.

3. Stone, G. W. (1994). *Projectile Penetration into Representative Targets*. SANDIA REPORT, 26 p.
4. Koene, L., & Broekhuis, F. R. (2017). *Bullet penetration into wooden targets.* 30th International Symposium on Ballistics, Long Beach, CA, 1905-1916.
5. Susu, L., Cheng, X., Yaoke, W., & Xiaoyun, Z. (2016). A new motion model of rifle bullet penetration into ballistic gelatin. *International Journal of Impact Engineering*, Volume 93, 1-10.
6. Saleh, M., Edwards, L., & Crouch, I. G. (2017). *Numerical modelling and computer simulations*. In the Science of Armour Materials, 483-579.
7. Belytschko, T., Gracie, R., & Ventura, G. (2009). A review of extended/generalized finite element methods for material modeling. *Modelling and Simulation in Materials Science and Engineering*, vol. 17, no. 4, Article ID 043001.
8. Kumar, B. A., & Ahmad, S. (2014). *A Ballistic Material Model for Kevlar Composite Targets*. Conference: 5th International Congress on Computational Mechanics and Simulation, 2432-2439.
9. Riedel, W., Thoma, K., Hiermaier, S., & Schmolinske, E. (1999). *Penetration of Reinforced Concrete by BETA-B-500 Numerical Analysis using a New Macroscopic Concrete Model for Hydrocodes*. Internationales Symposium, Interaction of the Effects of Munitions with Structures, Berlin Strausberg, 315-322.
10. Steinberg, D. J. (1996). *Equation of State and Strength Properties of Selected Materials*. LLNL report No. UCRL-MA-106439.
11. Shash, N., & Zuzov, V. N. (2017). Modified Johnson-Cook Model-based Numerical Simulation of Small Arms Bullets Penetration in the Aluminum Alloy Plates. *Science and Education of the Bauman MSTU*, no. 01, 1-19.
12. Richards, M., Clegg, R., & Howlett, S. (1999). *Ballistic performance assessment of glass laminates through experimental and numerical investigation.* Proceedings of the 18th International Symposium on Ballistics, 1123-1130.